muscle were implanted into the TA of irradiated *mdx nu/nu* mice, they formed a mean of 328 dystrophin-positive fibers (*5*). Similar results were obtained after injecting one to two million muscle-derived cultured cells into limb muscle (*2*, *3*). Our results now show that purified satellite cells are much more efficient than these crude or cultured cell populations in contributing to muscle repair.

The culture of muscle progenitor cells before grafting markedly reduces their regenerative efficiency such that the culture expansion itself is an "empty" process, yielding the same amount of muscle as the number of cells from which the culture was initiated. Culture-induced modifications may affect survival or engraftment capacity of the cells (*24*, *25*). However, we did not detect a difference in survival between cultured and freshly isolated cells 1 day after grafting (*23*). The activated state of the grafted cells may diminish their regenerative potential, because freshly isolated progenitor cells are not activated at the time of grafting, unlike their cultured progeny that express MyoD. Clonal assays suggest that the lower regenerative capacity of cultured cells reflects their more rapid differentiation. A similar situation is encountered with hematopoietic stem cells, which begin to differentiate and to lose their tissue reconstitution capacity when cultured (*26*).

Not only do purified muscle satellite cells contribute to muscle repair when engrafted into regenerating *mdx* muscles but some also persist as progenitor cells, adopting a satellite cell position and expressing Pax7. These results, therefore, point to muscle satellite cell self-renewal. The fact that (Pax3)GFP+ cells can be recovered from the muscles into which they were originally transplanted and shown to differentiate into muscle cells in culture also argues in favor of self-renewal. We therefore conclude that the satellite cell selection procedure described here results in cells that can both repair and contribute to the progenitor cell population of damaged muscles. There may be other stem cell types that can be mobilized to contribute to this process (*27*), but the muscle satellite cell population isolated by the flow cytometry parameters that we have defined is clearly a major contributor to muscle regeneration and a potential therapeutic agent.

References and Notes

1. S. B. Charge, M. A. Rudnicki, *Physiol. Rev.* **84**, 209 (2004).
2. Z. Qu-Petersen *et al.*, *J. Cell Biol.* **157**, 851 (2002).
3. G. M. Mueller, T. O'Day, J. F. Watchko, M. Ontell, *Hum. Gene Ther.* **13**, 1081 (2002).
4. D. Skuk, M. Goulet, B. Roy, J. P. Tremblay, *Exp. Neurol.* **175**, 112 (2002).
5. J. E. Morgan, C. N. Pagel, T. Sherratt, T. A. Partridge, *J. Neurol. Sci.* **115**, 191 (1993).
6. J. E. Morgan, R. M. Fletcher, T. A. Partridge, *Muscle Nerve* **19**, 132 (1996).
7. A. Irintchev, M. Zeschnigk, A. Starzinski-Powitz, A. Wernig, *Dev. Dyn.* **199**, 326 (1994).
8. A. Hollnagel, C. Grund, W. W. Franke, H. H. Arnold, *Mol. Cell. Biol.* **22**, 4760 (2002).
9. D. D. Cornelison, M. S. Filla, H. M. Stanley, A. C. Rapraeger, B. B. Olwin, *Dev. Biol.* **239**, 79 (2001).
10. J. R. Beauchamp *et al.*, *J. Cell Biol.* **151**, 1221 (2000).
11. P. Seale *et al.*, *Cell* **102**, 777 (2000).
12. M. Buckingham *et al.*, *J. Anat.* **202**, 59 (2003).
13. F. Relaix, D. Montarras, M. Buckingham, unpublished data.
14. F. Relaix, D. Rocancourt, A. Mansouri, M. Buckingham, *Nature* **435**, 948 (2005).
15. P. S. Zammit *et al.*, *J. Cell Biol.* **166**, 347 (2004).
16. Z. Yablonka-Reuveni, A. J. Rivera, *Dev. Biol.* **164**, 588 (1994).
17. D. D. Cornelison, B. J. Wold, *Dev. Biol.* **191**, 270 (1997).
18. J. C. van Deutekom, G. J. van Ommen, *Nat. Rev. Genet.* **4**, 774 (2003).
19. E. P. Hoffman, J. E. Morgan, S. C. Watkins, T. A. Partridge, *J. Neurol. Sci.* **99**, 9 (1990).
20. R. J. Jankowski, B. M. Deasy, B. Cao, C. Gates, J. Huard, *J. Cell Sci.* **115**, 4361 (2002).
21. R. I. Sherwood *et al.*, *Cell* **119**, 543 (2004).
22. I. M. Conboy, T. A. Rando, *Dev. Cell* **3**, 397 (2002).
23. D. Montarras *et al.*, unpublished data.
24. J. X. DiMario, F. E. Stockdale, *Exp. Cell Res.* **216**, 431 (1995).
25. J. R. Beauchamp, J. E. Morgan, C. N. Pagel, T. A. Partridge, *J. Cell Biol.* **144**, 1113 (1999).
26. J. Antonchuk, G. Sauvageau, R. K. Humphries, *Cell* **109**, 39 (2002).
27. T. Partridge, *Cell* **119**, 447 (2004).

28. We thank D. Rocancourt and C. Cimper for technical assistance. Supported by the Pasteur Institute and the CNRS, with additional grants from the Association Française contre les Myopathies, "the Cellules Souches" Grand Programme Horizontal of the Pasteur Institute, and the EuroStemCell Integrated Project of the European Union 6th Framework Programme. J.M., C.C., and T.P. received support from the Medical Research Council of the UK, the Muscular Dystrophy Campaign, and the Engineering and Physical Sciences Research Council. T.P. occupies a Blaise Pascal chair awarded by the Ecole Normale Supérieure. D.M. dedicates this paper to R. B. Seaver.

Supporting Online Material

www.sciencemag.org/cgi/content/full/1114758/DC1
Materials and Methods
Figs. S1 to S4
Table S1
References and Notes

12 May 2005; accepted 9 August 2005
Published online 1 September 2005;
10.1126/science.1114758
Include this information when citing this paper.

Regulation of Mammalian Tooth Cusp Patterning by Ectodin

Yoshiaki Kassai,[1]* Pauliina Munne,[2]* Yuhei Hotta,[1] Enni Penttilä,[2] Kathryn Kavanagh,[2] Norihiko Ohbayashi,[3] Shinji Takada,[3] Irma Thesleff,[2] Jukka Jernvall,[2,4]† Nobuyuki Itoh[1]†

Mammalian tooth crowns have precise functional requirements but cannot be substantially remodeled after eruption. In developing teeth, epithelial signaling centers, the enamel knots, form at future cusp positions and are the first signs of cusp patterns that distinguish species. We report that *ectodin*, a secreted bone morphogenetic protein (BMP) inhibitor, is expressed as a "negative" image of mouse enamel knots. Furthermore, we show that *ectodin*-deficient mice have enlarged enamel knots, highly altered cusp patterns, and extra teeth. Unlike in normal teeth, excess BMP accelerates patterning in *ectodin*-deficient teeth. We propose that *ectodin* is critical for robust spatial delineation of enamel knots and cusps.

Because cell differentiation and final pattern are directly linked in developing mammalian dentition, it is well suited for dissecting the molecular basis for induction and inhibition. The patterning of teeth involves iterative activation of the non-proliferative epithelial enamel knots at the places of future cusps (*1*, *2*). The surrounding epithelium and the underlying mesenchyme continue to proliferate, which results in folding of the epithelium to produce cusps (*1*, *3*). Spatial arrangements of cusps are typically species-specific and linked to evolution of diverse diets. Because erupted tooth crowns are fully mineralized, events during embryological patterning are critical for correct functional relations between occluding teeth. Consequently, classic studies have shown detailed coordination of development between occluding cusps (*4*), and that developing teeth are capable of self-regulation after external perturbations (*3*, *5*–*7*). This combination of precision and robustness of tooth development presumably extends to the placement of the secondary enamel knots as they are the earliest developmental signs of species-specific cusp patterns (*8*). Mathematical modeling has shown that, like feather patterning, an activator-inhibitor loop of signaling molecules could explain how the enamel knots determine

[1]Department of Genetic Biochemistry, Kyoto University Graduate School of Pharmaceutical Sciences, Kyoto 606-8501, Japan. [2]Developmental Biology Program, Institute of Biotechnology, Viikki Biocenter, Post Office Box 56, University of Helsinki, FIN-00014 Helsinki, Finland. [3]Okazaki Institute for Integrative Biosciences, National Institutes of Natural Sciences, Okazaki 444-8787, Japan. [4]Department of Ecology and Evolution, Stony Brook University, Stony Brook, NY 11794, USA.

*These authors contributed equally to this work
†To whom correspondence should be addressed. E-mail: itohnobu@pharm.kyoto-u.ac.jp (N.I.), jernvall@fastmail.fm (J.J.)

the morphological diversity seen in natural teeth (*9*). However, although not experimentally identified, this model suggested the existence of signaling molecules that inhibit the induction of the enamel knots.

Here we examined the functional role of *ectodin* (ectodermal inhibitor of BMP; GenBank accession number AB059271) in the regulation of mouse enamel knot formation following two lines of inquiry. First, we recently identified *ectodin* [the *Xenopus* ortholog is called *Wise* (*10*)] as a previously unknown protein (*11*) belonging to the Dan/Cerberus family of secreted BMP antagonists (*11*–*14*). We were interested in the inhibition of BMP signaling during tooth cusp patterning because the earliest differentiation marker of enamel knot cells, a cyclin-dependent kinase inhibitor *p21*, is induced by BMPs (*15*). The second reason for our interest in *ectodin* was that it seemed to be expressed around the primary enamel knot, forming at the onset of tooth crown formation, rather than in it (*11*). This kind of expression pattern, if it was to be repeated around the secondary enamel knots, would be the first of its kind (*16*).

Because histological sections of developing lower molars show complex expression patterns of *ectodin* (Fig. 1A), we analyzed gene expression in three dimensions. The results show that although *ectodin* is expressed in most parts of the forming first molar, the expression is absent in two distinct locations (Fig. 1B). The anterior (the trigonid) and posterior (the talonid) *ectodin*-negative regions contain secondary enamel knots, visible as the epithelial areas expressing *p21* (Fig. 1B). In mouse molar, the buccal and lingual cusps are joined by a transverse crest, and the areas forming these crests also express *p21* but not *ectodin* (Fig. 1B). In contrast, the area forming a valley separating the anterior and posterior cusp pairs expresses *ectodin* (Fig. 1B), suggesting inverse roles for *ectodin* and *p21* in cusp patterning. More distally, an *ectodin* expression domain separates the developing first and second molars, the latter being at the primary enamel knot stage of development (Fig. 1B). As in the first molar (*11*), the primary enamel knot in the second molar has no *ectodin* expression (Fig. 1, A and B).

The inverse expression patterns of *ectodin* and *p21* (Fig. 1B) are intriguing because both are induced by BMPs (*11*, *15*). BMPs are expressed in teeth throughout development (*17*), and mice lacking either type 1a BMP receptor in the epithelium (*18*) or, as a result of *Msx1*-null mutation, *Bmp4* expression in mesenchyme (*19*), have their tooth development arrested before primary enamel knot induction. Thus, although these mutants are indicative of the requirement of BMPs for tooth development, they leave the issue of cusp patterning unresolved. Furthermore, mice lacking functional *p21* have no reported tooth phenotypes (*20*), presumably as a result of redundancy with other cyclin-dependent kinase inhibitors. Ectodin, as an antagonist binding to BMPs (*11*), could be a feedback inhibitor of cusp development by interfering with the induction of *p21*. We first confirmed this by introducing ectodin-soaked beads together with BMP4-soaked beads on dental epithelium (*21*). Whereas BMP4 was sufficient to induce *ectodin* and *p21* in isolated dental epithelium, ectodin inhibited BMP4-induced *p21* expression (fig. S1).

We next investigated regulation of enamel knots by generating *ectodin*-deficient mice (*21*) (fig. S2). Although the overall development of teeth appears fairly normal in *ectodin*-deficient mice, tooth morphologies are highly altered. Changes in cusp patterns become visible as soon as *p21* is up-regulated in the developing secondary knots. The results show enlarged expression domains of *p21* with diminished intercuspal regions in the anterior portion of the first molar (Fig. 1C). Analyses of other enamel knot marker genes confirm that the induction of the enamel knot fate took place at the expense of intercuspal tissue (fig. S3). The distal *p21* expression domain of the first molar extends without interruption to the area normally giving rise to the second molar with no clear morphological separation between these teeth (Fig. 1, B and C). Accordingly, in erupted tooth rows of *ectodin*-deficient mice, the first and the second molars were often fused (21/52 = 40%).

An extra molar forms anterior to the first molar in the *ectodin*-deficient mice (Figs. 1C and 2). This tooth appears to develop slightly faster than the more posterior teeth and, at day 16, the whole crown expresses *p21* (Fig. 1C). To explore its developmental origin, we examined earlier stages using sonic hedgehog (*Shh*) expression as a marker for dental placodes. The results indicate that the extra tooth develops from a separate placode anterior to the first molar (Fig. 2A). Compared to the

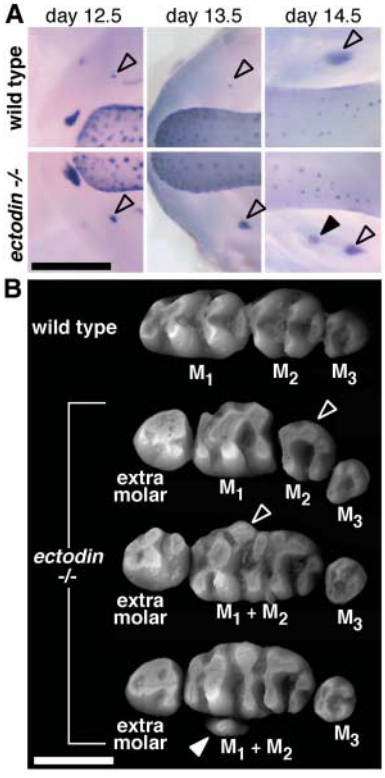

Fig. 2. *Ectodin*-deficient mice have extra teeth, fused molars, and highly altered cusp patterns. (**A**) The molar placodes indicated by *Shh* expression (open arrowhead) were larger in *ectodin*-null mutants than those in wild-type littermates, and at embryonic day 14.5, extra placodes (black arrowhead) appear anteriorly to the forming molars. (**B**) Three-dimensional laser confocal scans revealed that erupted tooth crowns of *ectodin*-deficient mice are broader than wild-type molars, have well-developed transverse crests, and have fused buccal cusps forming an ectoloph (open arrowhead). Extra cusps fused with the ectoloph, a lingual peg-shaped extra tooth (white arrowhead), and fused first and second molars are also observed. Anterior side is toward the left and buccal side is toward the top (B); M_1, first lower molar; M_2, second lower molar; M_3, third lower molar; $M_1 + M_2$, fused molars. Scale bars, 1 mm.

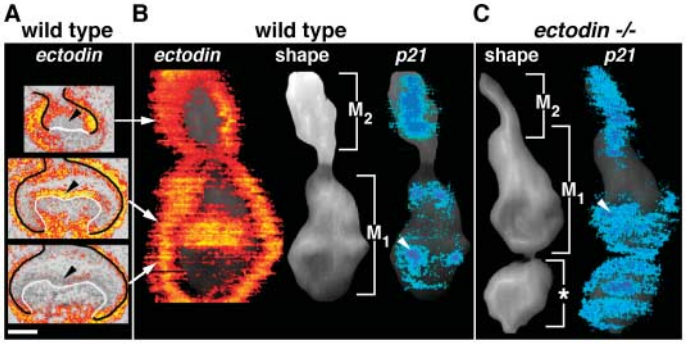

Fig. 1. *Ectodin* is expressed around the enamel knots and *ectodin* deficiency causes expansion of *p21* expression domains. (**A**) Frontal sections of embryonic day 16 mouse lower molars show complex patterns of *ectodin* expression in the forming tooth crown (black arrowheads). (**B**) Three-dimensional reconstructions show that ectodin is expressed around the enamel knots that express *p21* [occlusal views of the inner enamel epithelium marked with a white line in (A)]. (**C**) *Ectodin*-deficient mice show enlarged *p21* expression domains with decreased separation between forming cusps and molars. White arrowhead in (B) and (C) mark the secondary enamel knot forming the protoconid cusp, and asterisk in (C) marks an extra molar anterior to the first molar. Anterior side is toward the bottom (B and C) and buccal side is toward the left; M_1, first lower molar; M_2, second lower molar. Scale bar, 100 μm.

second molar, which develops as an early posterior extension of the first molar, the separate origin of the extra tooth conforms to the lack of fusion with the first molar. Similarities in placodes expressing *Shh* also suggest that the extra molar in *ectodin*-deficient mice is the same as that in mice that overexpress *ectodysplasin* (*22*). It remains to be shown whether ectodin and ectodysplasin function in the same or in parallel pathways regulating placode development.

To study cusp patterns of the *ectodin*-deficient mice, we used high-resolution three-dimensional laser-confocal imaging (*22*). Although most aspects of tooth crowns are affected (Fig. 2B), the most pronounced change was in the buccal side of the crowns. Indicating decreased down-growth of valleys separating cusps, the buccal side had better developed connections or completely fused cusps anterior-posteriorly, forming a longitudinal crest with fused extra cusps (Fig. 2B). This phenotype is reminiscent of the ectoloph, a feature present in, for example, the upper molars of black rhinoceros (resemblance of "*ectodin*" to this classic morphological term is coincidental). This buccal bias is noteworthy because *Bmp4* (*17*), *ectodin*, and *p21* (Fig. 1) are all expressed strongly in the buccal side, and our results may suggest a role for regulation of ectodin in the evolution of lateral bias in teeth. Despite the extensively derived morphology, the *ectodin*-deficient teeth are functional and individual mice do not seem to have occlusal problems with their molar teeth.

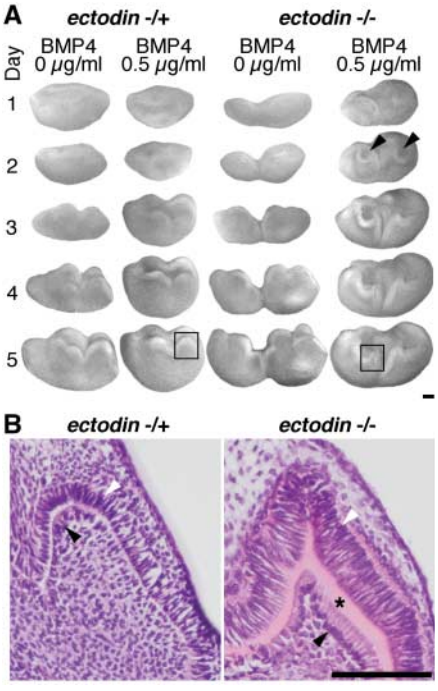

Fig. 3. Ectodin deficiency increases the sensitivity of developing teeth to excess BMP. Cap stage (day 14) teeth of *ectodin* heterozygous and null mutant embryos were cultured with BMP4 in the culture medium for the first 2 days. (**A**) (Left) BMP4 has little effect on tooth development of ectodin heterozygotes, and cusps appear normally during the third day of culture. (Right) In the *ectodin*-null mutants, which develop both the extra and the first molar, cusps are visible by the second day of culture with BMP4 (black arrowheads). The resulting crowns have sharp cusps, and all crowns were covered by dentine after 5 days of culture. (**B**) Histological sections of the regions in the black rectangles in (A) show that ectodin-null mutants cultured with BMP4 have fully polarized ameloblasts (white arrowhead) and odontoblasts (black arrowhead) that have already secreted a layer of dentine (asterisk). In heterozygote teeth cultured with BMP4, ameloblasts and odontoblasts are only starting to elongate. Some teeth cultured without BMP4 have begun to secrete dentine on cusp tips (not shown). All teeth (n = 28) were from the same homozygous-heterozygous crossing. Anterior side is toward the left (A). Scale bars, 100 μm.

Although the phenotype and enlarged enamel knots of the *ectodin*-deficient teeth are strongly suggestive about the role of ectodin in inhibiting enamel knot induction, these results do not directly implicate inhibition of BMP signaling. Next, to test the association of ectodin with BMP signaling in tooth crown development, we exposed *ectodin*-deficient teeth to BMP in culture.

We cultured isolated molars of both *ectodin* null-mutants and heterozygotes, which have wild-type dentition, with BMP4 in the culture medium for the first 2 days (*21*). The results show that in the absence of BMP4, the rates of tooth development of both null mutants and heterozygotes are similar (Fig. 3A). Whereas *ectodin* heterozygous teeth are not particularly sensitive to excess BMP4, the null-mutants show a markedly accelerated crown development, exceeding the rate of normal development in vivo by about 3 days (Fig. 3A). Already after 1 day in culture the null-mutant teeth show cusps and thickening of inner enamel epithelium (Fig. 3A). After 5 days of culture, ameloblasts and odontoblasts are fully differentiated in the null-mutants and the crowns are covered by dentine (Fig. 3B). Compared to both feather and limb patterning, which can be manipulated by BMPs (*23*–*26*), our present results, together with our earlier observations (*27*, *28*), suggest that normal tooth patterning is relatively robust against excess BMP.

Taken together, our results indicate that although the morphology of the *ectodin*-deficient teeth results from shifting the balance of induction toward larger enamel knots (Figs. 1 and 2), the systemic effect of lack of ectodin is the loss of self-regulation (Fig. 3). Thus, excess BMP administered to developing *ectodin*-deficient teeth caused relatively unchecked induction. In contrast, in normal teeth the cusp induction and inhibition cascades cancel each other out under excess BMP. Uniquely in mammals, once erupted, permanent dentition must last the whole lifetime of the animal. This alone suggests that there has been strong selective pressure to make tooth development as "fail-proof" as possible, and we propose that robustness of tooth development to external perturbations requires ectodin to integrate cusp induction and inhibition.

Although *ectodin*-deficient mice have the most extensively modified cusp patterns of mouse mutants studied to date, mice with superfluous production of *ectodysplasin* have some similarities with *ectodin*-deficient mice. Both have extra teeth and longitudinal crests connecting cusps. However, the *ectodin*-deficient mice have buccal crests (Fig. 2B), whereas mice overexpressing *ectodysplasin* have central crests (*22*). This single difference in morphology is enough to alter the mutant phenotypes to resemble rhinoceros and kangaroo teeth, respectively. These morphological alterations, although functional, are obviously larger than evolutionary transitions documented in the fossil record. Hence, it remains to be determined whether fine tuning of enamel knot formation could be sufficient, perhaps by allelic changes as shown for *ectodysplasin* in altering armor plates of sticklebacks (*29*), to account for the evolutionary diversity of teeth.

References and Notes

1. J. Jernvall, P. Kettunen, I. Karavanova, L. B. Martin, I. Thesleff, *Int. J. Dev. Biol.* **38**, 463 (1994).
2. J. Jernvall, I. Thesleff, *Mech. Dev.* **92**, 19 (2000).
3. P. M. Butler, *Biol. Rev.* **31**, 30 (1956).
4. P. M. Marshall, P. M. Butler, *Arch. Oral Biol.* **11**, 949 (1966).
5. S. Glasstone, *Proc. R. Soc. Lond. B. Biol. Sci.* **126**, 315 (1939).
6. S. Glasstone, *J. Dent. Res.* **42**, 1364 (1963).
7. A. R. Fisher, *Arch. Oral Biol.* **16**, 1481 (1971).
8. J. Jernvall, S. V. E. Keränen, I. Thesleff, *Proc. Natl. Acad. Sci. U.S.A.* **97**, 14444 (2000).
9. I. Salazar-Ciudad, J. Jernvall, *Proc. Natl. Acad. Sci. U.S.A.* **99**, 8116 (2002).
10. N. Itasaki *et al.*, *Development* **130**, 4295 (2003).
11. J. Laurikkala, Y. Kassai, L. Pakkasjarvi, I. Thesleff, N. Itoh, *Dev. Biol.* **264**, 91 (2003).
12. W. Balemans, W. Van Hul, *Dev. Biol.* **250**, 231 (2002).
13. N. Kusu *et al.*, *J. Biol. Chem.* **278**, 4113 (2003).
14. O. Avsian-Kretchmer, A. J. Hsueh, *Mol. Endocrinol.* **18**, 1 (2004).
15. J. Jernvall, T. Åberg, P. Kettunen, S. Keränen, I. Thesleff, *Development* **125**, 161 (1998).
16. http://bite-it.helsinki.fi/
17. T. Åberg, J. Wozney, I. Thesleff, *Dev. Dyn.* **210**, 383 (1997).
18. T. Andl *et al.*, *Development* **131**, 2257 (2004).
19. Y. Chen, M. Bei, I. Woo, I. Satokata, I. R. Maas, *Development* **122**, 3035 (1996).
20. C. Deng, P. Zhang, J. W. Harper, S. J. Elledge, P. J. Leder, *Cell* **82**, 675 (1995).
21. Materials and methods are available as supporting material on *Science* Online.
22. A. T. Kangas, A. R. Evans, I. Thesleff, J. Jernvall, *Nature* **432**, 211 (2004).
23. H.-S. Jung *et al.*, *Dev. Biol.* **196**, 11 (1998).
24. S. Noramly, B. A. Morgan, *Development* **125**, 3775 (1998).
25. R. Merino *et al.*, *Development* **126**, 5515 (1999).
26. J. Selever, W. Liu, M. F. Lu, R. R. Behringer, J. F. Martin, *Dev. Biol.* **276**, 268 (2004).
27. J. Jernvall, H.-S. Jung, *Yearb. Phys. Anthropol.* **43**, 171 (2000).
28. Y. Kassai *et al.*, data not shown.
29. P. F. Colosimo *et al.*, *Science* **307**, 1928 (2005).

30. This work was supported by a Grant-in-Aid for

Creative Scientific Research (N.I.) and the 21st Century Centers of Excellence Program (Y.K.) from the Ministry of Education, Culture, Sports, Science and Technology of Japan; a grant from the Mitsubishi Foundation, Japan (N.I.); the Finnish Academy (J.J., I.T.); and the Sigrid Juselius Foundation (I.T.). We thank A. Evans, H. Kettunen, M. Mäkinen, I. Salazar-Ciudad, R. Santalahti, and P. C. Wright for comments or technical help.

Supporting Online Material
www.sciencemag.org/cgi/content/full/309/5743/2067/DC1
Materials and Methods
Figs. S1 to S3

1 July 2005; accepted 23 August 2005
10.1126/science.1116848

Genetic Engineering of Terpenoid Metabolism Attracts Bodyguards to *Arabidopsis*

Iris F. Kappers,[1,2]* Asaph Aharoni,[2,3]* Teun W. J. M. van Herpen,[2] Ludo L. P. Luckerhoff,[1,2] Marcel Dicke,[1] Harro J. Bouwmeester[2]†

Herbivore-damaged plants release complex mixtures of volatiles that attract natural enemies of the herbivore. To study the relevance of individual components of these mixtures for predator attraction, we manipulated herbivory-induced volatiles through genetic engineering. Metabolic engineering of terpenoids, which dominate the composition of many induced plant volatile bouquets, holds particular promise. By switching the subcellular localization of the introduced sesquiterpene synthase to the mitochondria, we obtained transgenic *Arabidopsis thaliana* plants emitting two new isoprenoids. These altered plants attracted carnivorous predatory mites (*Phytoseiulus persimilis*) that aid the plants' defense mechanisms.

The integration of ecology and molecular biology has yielded important progress in understanding complex interactions between organisms and the underlying mechanisms (*1*). In recent years, *Arabidopsis thaliana* L. was shown to be an excellent model plant for investigating ecological interactions such as induced indirect defense. In these tritrophic interactions, plants defend themselves against feeding by herbivorous arthropods by producing volatiles that attract the natural enemies of the herbivores (*2*–*4*). The activities of these natural enemies benefit the plant's fitness, and this defense therefore is evolutionarily advantageous (*5*–*7*). Hence, the term "bodyguard" has been used to describe the function of carnivorous arthropods such as predatory mites (*5*). For example, feeding by caterpillars of the crucifer pest *Pieris rapae* resulted in the emission of volatiles that attracted the parasitoid wasp *Cotesia rubecula* (*8*, *9*). The parasitization of *P. rapae* caterpillars by *C. rubecula* resulted in an increase in plant fitness in terms of seed production and thus benefited the plant (*7*). The individual components of herbivore-induced volatile blends originate from various chemical classes, but isoprenoids dominate the composition of many of these blends (*10*–*13*) and are known to attract carnivorous arthropods (*2*–*14*). One of the herbivore-induced volatiles in *Arabidopsis* is the C16-homoterpene 4,8,12-trimethyl-1,3(*E*),7(*E*),11-tridecatetraene [(*E*,*E*)-TMTT)] (*8*). A related compound, the C11-homoterpene 4,8-dimethyl-1,3(*E*),7-nonatriene [(*E*)-DMNT], has been detected in the headspace of many plant species after herbivory (*12*, *14*, *15*), but not in the (induced or noninduced) volatile mixture of *Arabidopsis* (*8*, *16*).

Our first step in studying the ecological relevance of individual compounds of the complex herbivory-induced volatile mixture was to generate transgenic plants that constitutively emit these chemicals. We chose to engineer the sesquiterpene (3*S*)-(*E*)-nerolidol, a component of the herbivore-induced volatile blend of, for example, maize (*17*) and tomato (*18*) and the first dedicated intermediate en route to (*E*)-DMNT (*15*, *17*) (Fig. 1A). Earlier attempts to produce substantial amounts of sesquiterpenes in transgenic plants failed, most probably because of a lack of sufficient precursors (*19*–*21*). In these experiments, sesquiterpene synthases were targeted either to the cytosol (*19*, *20*)—which is the expected location of farnesyl diphosphate (FPP), the precursor for sesquiterpenes—or to the plastids (*21*). Here, we targeted FaNES1, a strawberry linalool/nerolidol synthase, specifically to the mitochondria. We reasoned that because the mitochondria are the site of ubiquinone biosynthesis and *Arabidopsis* possesses an FPP synthase isoform with a mitochondrial targeting signal (*22*, *23*), FPP should be available in this cell compartment.

The CoxIV (cytochrome oxidase subunit IV) sequence, a bona fide mitochondrial targeting signal (*24*), was used to localize FaNES1 to the mitochondria (*25*). Transgenic *Arabidopsis* plants harboring the CoxIV-FaNES1 construct (Fig. 1B) were generated, and *FaNES1* expression was detected in leaves of primary transformants (Fig. 1C). In earlier work we showed that in protoplasts, CoxIV when fused to green fluorescent protein (GFP) efficiently targeted GFP to the mitochondria (*26*). The headspace of rosette leaves from 4-week-old plants was analyzed using solid-phase microextraction (SPME) as described (*21*), and 9 of

[1]Laboratory of Entomology, Wageningen University, Post Office Box 8031, 6700 EH Wageningen, Netherlands. [2]Plant Research International, Wageningen University and Research Centre, Post Office Box 16, 6700 AA Wageningen, Netherlands. [3]Weizmann Institute of Science, Post Office Box 26, Rehovot 76100, Israel.

*These authors contributed equally to this work.
†To whom correspondence should be addressed. E-mail: harro.bouwmeester@wur.nl

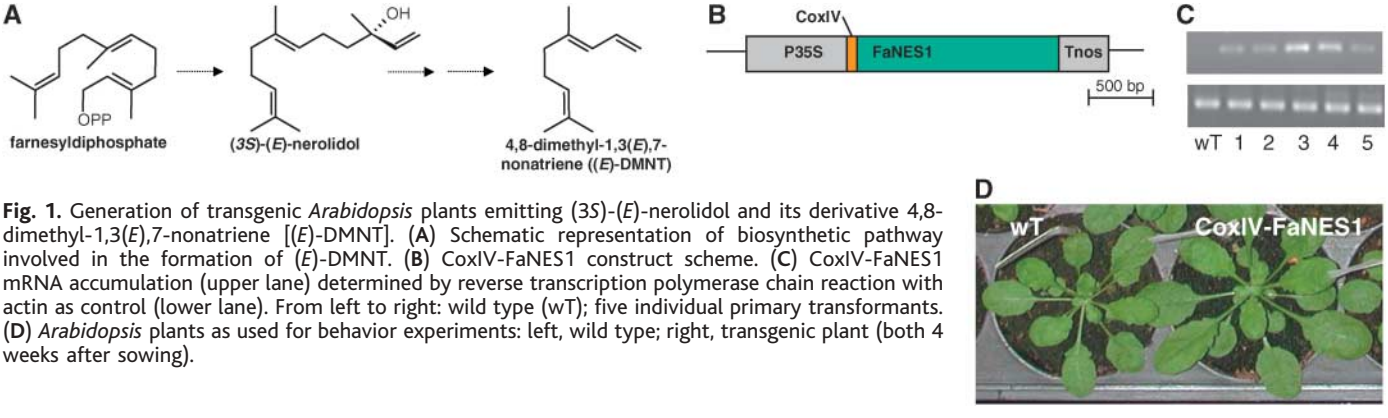

Fig. 1. Generation of transgenic *Arabidopsis* plants emitting (3*S*)-(*E*)-nerolidol and its derivative 4,8-dimethyl-1,3(*E*),7-nonatriene [(*E*)-DMNT]. (**A**) Schematic representation of biosynthetic pathway involved in the formation of (*E*)-DMNT. (**B**) CoxIV-FaNES1 construct scheme. (**C**) CoxIV-FaNES1 mRNA accumulation (upper lane) determined by reverse transcription polymerase chain reaction with actin as control (lower lane). From left to right: wild type (wT); five individual primary transformants. (**D**) *Arabidopsis* plants as used for behavior experiments: left, wild type; right, transgenic plant (both 4 weeks after sowing).